



## Article

# Simulation of *Prosopis juliflora* Air Gasification in Multistage Fluidized Process

Maryem Dhrioua <sup>1</sup>, Walid Hassen <sup>1</sup>, Lioua Kolsi <sup>2,\*</sup>, Kaouther Ghachem <sup>3</sup>,  
Chemseddine Maatki <sup>4</sup> and Mohamed Naceur Borjini <sup>1</sup>

<sup>1</sup> Research Laboratory of Metrology and Energy Systems, National Engineering School of Monastir, University of Monastir, Monastir 5000, Tunisia; maryemdhrioua@gmail.com (M.D.); hassan.walid@gmail.com (W.H.); borjinimn@yahoo.com (M.N.B.)

<sup>2</sup> Department of Mechanical Engineering, College of Engineering, University of Ha'il, Ha'il City 81481, Saudi Arabia

<sup>3</sup> Department of Industrial Engineering and Systems, College of Engineering, Princess Nourah Bint Abdulrahman University, Riyadh 84428, Saudi Arabia; kgmaatki@pnu.edu.sa

<sup>4</sup> Department of Mechanical Engineering, College of Engineering, Al Imam Mohammad Ibn Saud Islamic University, Riyadh 11432, Saudi Arabia; maatkichems@yahoo.fr

\* Correspondence: l.kolsi@uoh.edu.sa or lioua\_enim@yahoo.fr

Received: 17 November 2020; Accepted: 10 December 2020; Published: 15 December 2020



**Abstract:** A multistage atmospheric fluidized bed gasifier was developed using the Aspen Plus simulation process. The innovative gasification reactor aims to yield a high-quality product gas as it conducts pyrolysis, combustion, and reduction in different zones. In addition, it uses gas as a heat carrier and has a fluidized char bed in the reduction zone to enhance the in-situ tar reduction. In order to study the feasibility of the gasifier, an evaluation of the product gas and the process efficiency is required. The proposed model was based on the reaction rates and hydrodynamic parameters of the bubbling bed. Four different stages were initially considered in the simulation process: decomposition of the feed, partial volatile combustion, char reduction, and gas solid separation. The gasification reactor was operated over a temperature range of 800–1000 °C and an isothermal combustion reactor was operated at 1000 °C. In addition, the air to biomass mass ratio was varied from 0.2 to 0.5. It has been validated and displayed very good agreement with published data. Effects of gasification reactor temperature, air to biomass ratio, and gasifier dimensions on the composition of product gas were investigated. Results showed that the principal component is CO and its concentration in the product gas increases with increase in gasifier temperature but decreases with increasing air to biomass ratio. The results also gave a relatively high value of the lowered gas caloric value and acceptable cold gas efficiency which help the sizing of gasifiers and the choice of optimal operating conditions.

**Keywords:** fluidized-bed; multistage gasifier; Aspen Plus

## 1. Introduction

Biomass is characterized by its diversity, abundance, and renewability. It is accordingly considered one of the most important sources of renewable energy [1]. It is an important renewable energy source as it helps with the increasing energy utilization in addition to satisfying the requirements of sustainable development with near zero CO<sub>2</sub> emissions [2,3]. Biomass gasification has gained worldwide attention thanks to its high energy conversion efficiency as well as its ability to operate with important ranges of biomass feedstocks. It is a thermo-chemical process that uses heat, involving pyrolysis, combustion, and reduction, to convert biomass into producer gas/synthesis gas (syngas) through a series of heterogeneous and homogeneous reactions. Synthesis gas usually contains H<sub>2</sub>, CO, CH<sub>4</sub>, N<sub>2</sub>, and other

undesirable components such as CO<sub>2</sub> and tar, and can be used for different purposes: generation of other valuable products for the chemical industry as well as power and heat [4].

Several factors can affect the composition of product gas and the concentration of its impurities [5], such as the reactor design, the gasifying agent and its velocity, the temperature of the reactor, etc. In fact, biomass gasification can occur in typical single stage reactors or in multistage ones. Depending on the gas velocity, gasification can take place in different regimes, for instance, fixed bed, bubbling bed, and circulating bed. Loha et al. [6] stated that fluidized beds are preferred for the gasification of biomass as they promote the solid feedstock conversion by an excellent mixing and contact between gas and solid particles. In addition, integrating char in the fluidized bed can be used as an effective means for tar decomposition, as stated by Basu [4]. There are many researchers [7–9] who investigated the effect of multistage gasification systems and they affirmed that they upgraded the quality of the product gas by diminishing the tar concentration. Therefore, an exclusive gasification technology, a multistage fluidized bed gasifier, that aims at low tar production could be developed on the basis of the above-mentioned principles.

Several researchers have focused on modeling biomass gasification using the Aspen Plus simulator in order to study and determine the optimal composition of the produced gas. In addition, the development of gasification reactors generally needs different levels of material and human resources. Therefore, using computer simulations is the efficient way to solve this problem. The Aspen Plus simulator is a program process that can be used to compute mass and energy balances dealing with multiphase models. It is used in the simulation of a diversity of processes like fluidized-beds and gasification reactors [10]. The performance analysis of fluidized beds for biomass gasification can be studied using thermodynamic equilibrium or kinetic modeling [11]. Two different thermodynamic models employing Gibbs energy minimization have been used by different researchers [11]. Thermodynamic equilibrium models do not consider the hydrodynamics of the process. They are independent of the gasifier type, unlike thermodynamic semi-equilibrium models which provide better prediction of producer gas composition. The kinetic models take into consideration both the hydrodynamic behavior and the reaction kinetics to make it the physically most realistic model. Mallick et al. [11] stated that this approach is very important when it comes to designing, improving, and evaluating gasification systems. Most of the studies did not consider tar, or loaded it over other heavy hydrocarbons [12]. Some others considered it as chemically inert, so it did not take part in the chemical reactions [13]. Regarding pyrolysis, some researchers [6] considered it as an instantaneous process. According to this assumption, the pyrolysis compositions can be used as inputs in gasification simulations.

Niu et al. [14] focused on a comprehensive modeling using Aspen Plus to simulate the solid waste gasification inside a fluidized bed gasifier. They stated that the production of CO and H<sub>2</sub>, and the gasification efficiency were improved as a result of the increase of gasification temperature. Doherty et al. [15] used the Aspen Plus simulator to study a fluidized bed process. Their model was also based on Gibbs free energy minimization. They found that syngas composition and heating value were strongly influenced by both gasification temperature and steam to biomass ratio. In addition, it was stated that cold gas efficiency was affected by the biomass moisture. Likewise, on the basis of Gibbs free energy minimization, Sreejith et al. [16] developed a steam gasification biomass model using the Aspen Plus simulator. Their study was based on an equilibrium model based on Gibbs free energy minimization and aimed to determine the optimum process conditions of gasification. Using the same model, Begum et al. [3] developed an Aspen Plus model to study different biomass feedstocks' gasification. It is about a fixed bed integrated gasifier that predicted the model's steady state performances. The authors could provide the optimum performance for the feedstocks studied. Mitta et al. [17] presented a model for a fluidized bed type gasification process. Their study focused on the effect of the flow rate, the temperature and composition of the feed material, and the operating pressure and temperature. The developed model was able to predict the composition of the produced gas and the effect of operating temperature on the gas composition.

Beheshti et al. [18] simulated the air–steam biomass gasification to produce hydrogen and syngas. They used an Aspen Plus model based on chemical reaction rates and hydrodynamic properties: a semi detailed kinetic model. Empirical correlations of pyrolysis yields were used. They studied and discussed the effects of some critical parameters like gasification temperature, biomass particle size, steam to biomass ratio, and equivalence ratio on the composition of the gas produced. Abdelouehed et al. [19] studied biomass gasification in dual fluidized beds. They modeled the process by Aspen Plus using a semi detailed kinetic mechanism. In their work, pyrolysis products were calculated through correlations and were considered as feeds to other reactors. Their model predictions for methane and tar yields were in agreement with data of pilot plants. They stated that the semi detailed kinetic model can be used to optimize biomass gasifier performances.

The present work focuses on gasification modelling using a semi detailed kinetic model in the Aspen Plus Simulator. The innovation points of the multistage gasifier studied are the design and the usage of a fluidized bed in the reduction zone to produce a high-quality product gas. This reactor has been studied in CFD cold model. The novelty of this study is to develop a numerical tool that introduces species and chemical reactions in order to investigate the main product gas composition, lower heating value (LHV), and cold gas efficiency (CGE), depending on the variation of gasification temperature and bed material. The hydrodynamics of the bed were investigated as well.

## 2. Process Modeling

### 2.1. Concept of the Multistage Gasifier

As presented in Figure 1a, the considered system comprises three different stages: pyrolysis, combustion, and reduction. Details of the system are in the previous work of Dhrioua et al. [20]. Initially, biomass is heated inside the pyrolysis reactor to yield char and pyrolytic gas. They will be separated and fed to reduction and combustion zones, respectively. The hot gas generated after the oxidation of pyrolysis gas will be the fluidizing and gasification agent of the reduction zone's fluidized bed. The reduction reactions will generate the product gas (estimated at 800–1000 °C) that will be conducted to the pyrolizer jacket to deliver the necessary heat for the pyrolysis zone. Therefore, compared to a classical dual fluidized bed reactor, instead of burning char, it will be used for reduction by the hot gases generated from burning the pyrolysis gas. The purpose of this process is to present an exclusive gasification technology with low tar production in addition to the use of a fluidized bed as a means to fuel flexibility.

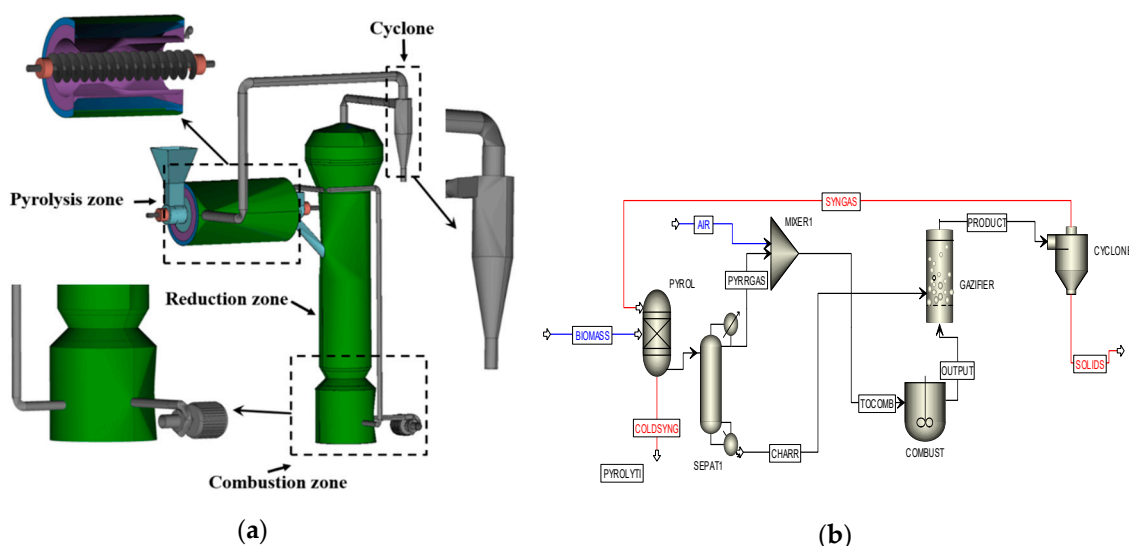


**Figure 1.** (a) 3D schematic of the multistage gasifier and (b) flowsheet of the Aspen Plus model.

## 2.2. Process Assumptions

The biomass devolatilization is an instant process resulting principally in CO, CO<sub>2</sub>, CH<sub>4</sub>, H<sub>2</sub>, and H<sub>2</sub>O. The gases obtained in the devolatilization step are used as inflows of the gasifier and combustor. In fact, pyrolysis contains tremendously complex reactions, and a feasible methodology is the use of pyrolysis products as an input in the succeeding steps [19]. Considering the work of Chandrasekaran et al. [21], the optimal conditions of the pyrolysis of *Prosopis juliflora* (PJ) are: particle size of biomass between 0.2 to 0.5 mm, pyrolysis temperature 600 °C, and heating rate of 20 °C/min. This will produce a mass rate of char = 21%, gas = 45.4%, and liquid (bio-oil) = 33.6%. The corresponding composition of the gas is: CO = 38%; CO<sub>2</sub> = 28%; H<sub>2</sub> = 16.5%; CH<sub>4</sub> = 17.5%. In this model, the presence of tar is not considered to simplify the model. Char is assumed to be 100% carbon and ash does not contribute to chemical reactions as it is assumed to be inert.

The following supplementary assumptions are considered: isothermal and steady state processes are supposed in both the combustion and gasification reactors. The solids are perfectly mixed, and the bed is bubbling. Char reduction begins in the bubbling bed and is completed in the freeboard zone. A constant average particle diameter is considered during the process and N<sub>2</sub> is supposed to be inert. Table 1 summarizes assumptions and desired design conditions.

**Table 1.** Assumptions and Desired Design Conditions.

Type of Gasifier	Multistage Bubbling Fluidized
Type of Fuel	<i>Prosopis juliflora</i>
Calorific value of Fuel	17 MJ/kg
Fuel consumption rate	10 kg/h
Syngas components	CO, H <sub>2</sub> , CO <sub>2</sub> , CH <sub>4</sub> and N <sub>2</sub> (800–1000 °C)
Char formula	Black Carbon
Gasification reactor	Cylindrical (H:2–4 m, D:0.35–0.55 m) isothermal (800–1000 °C)
Combustion reactor	Volume: 0.3 m <sup>3</sup> , isothermal: 1000 °C
Pyrolysis products (%vol) [21]	T = 600 °C: 21% Char, 33.6% liquid, 45.4% gas (0.38 CO, 0.175 CH <sub>4</sub> , 0.165 H <sub>2</sub> , 0.28 CO <sub>2</sub> )
Distributor	Perforated plate: perforated area 0.125–1.25%
Air feed	T = 25 °C: 2–5 kg/h
Bed solid diameter [21]	200–500 µm
Desired LHV	>10 MJ/Nm <sup>3</sup>
Desired Cold Gas Efficiency (CGE)	>60%

## 2.3. Aspen Plus Process Modeling

In this section, air gasification of *Prosopis juliflora* has been modeled by adopting a detailed kinetic Aspen Plus process. Figure 1b illustrates the Aspen flowsheet of the present process. The entire procedure contains four distinct stages: decomposition of the biomass, gas solid separation, partial volatile combustion, and char gasification. A semi detailed kinetic scheme is used. An isothermal RYIELD reactor; called PYROL (Figure 1b) is employed for the simulation of the pyrolysis process. Pyrolysis yields considered are sent to the separation column (Separ1). This pyrolysis gas is mixed with air at the beginning of the partial combustion process. Gas combustion occurs in the “Combustor” which is an Aspen Plus RCSTR reactor that performs perfect mixing gas combustion. Consequently, the reactor substances have identical compositions and properties at the outlet flow.

After burning all the oxygen, the process of gasification begins. Char gasification occurs in the “Gasifier” which is an Aspen Plus Fluidized reactor performing char gasification by using reaction kinetics. This FLUIDBED Aspen Plus block will be described in the following. After this, a cyclone is used to separate solids from the producer gas. Then syngas is used as a heat source for the RYIELD pyrolysis reactor. In Aspen Plus, the Fluidbed Block is a recently added library model reactor module that is used to model fluidized beds. In the following, we give specifications of the fluidized bed module: reactor model assumptions, configuration, and operational conditions. In addition, the gas distributor’s

specifications, i.e., type and holes' dimensions are also specified in this module. The fluidized bed is separated into bottom and upper zones that are categorized by a high concentration of solid volume, and a diminished concentration with increasing height, respectively. They are modeled as bubbling bed and dilute zone.

- Minimum fluidization velocity ( $U_{mf}$ )

Aspen Plus software computes minimum fluidization velocity by the Equation (1) given by Ergun:

$$u_{mf} = 7.14 \cdot (1 - \varepsilon_{mf}) \cdot \gamma_g \cdot S_v \cdot \left[ \sqrt{1 + 0.067 \cdot \frac{\varepsilon_{mf}^3}{(1 - \varepsilon_{mf})^2} \cdot \frac{(\rho_s - \rho_g) \cdot g}{\rho_g \cdot \gamma_g^2} \cdot \frac{1}{S_v^3}} - 1 \right] \quad (1)$$

where  $\rho_g$ ,  $\gamma_g$  are gas density and dynamic viscosity,  $\rho_s$  particle density,  $\varepsilon_{mf}$  bed porosity at minimum fluidization, and  $S_v$  volume-specific surface area.

- Superficial gas velocity

The superficial gas velocity is then given by Equation (5):

$$u_g(h) = \frac{m_g(h)}{\rho_g(T, p(h)) A(h)} \quad (2)$$

- Pressure drops:

- across the bed:

$$\Delta p_{fb} = H(1 - \varepsilon) \rho_s g + H \varepsilon \rho_g g \quad (3)$$

- across the distributor:

$$\Delta p_{dis} = \left( \frac{u_{or}}{C_{dis}} \right)^2 \frac{\rho_g}{2} \quad (4)$$

The model of Geldart et al. [22] is chosen for elutriation. More details on this model can be found in Aspen Plus Simulator Help and in the descriptions by Hussain et al. [23]. Lower heating value (LHV) and cold gas efficiency (CGE) [24]:

$$LHV_{fuel} = 33.9 Y_c + 102.9 Y_H - 11.2 Y_O - 2.5 Y_{H_2O} \text{ [MJ/kg]} \quad (5)$$

where  $Y$  is the mass fraction of each specie. The calculated LHV of *Prosopis juliflora* fuel is about 17 MJ/kg [21].

The producer gas lower heating value ( $LHV_{gas}$ ) can be determined by [24]:

$$LHV_{Gas} = 12.64 X_{CO} + 10.8 X_{H_2} + 35.8 X_{CH_4} \text{ [MJ/Nm}^3\text{]} \quad (6)$$

where  $X$  is the mole fraction of each specie.

Cold gas efficiency (CGE) is determined by:

$$CGE = \frac{LHV_{gas} V_{gas}}{LHV_{Fuel} m_{Fuel}} \quad (7)$$

where  $V_{gas}$  is syngas volumetric flow rate,  $m_{fuel}$  is the fuel mass flow rate,  $LHV_{gas}$  is the syngas lower heating value, and  $LHV_{fuel}$  is the fuel lower heating value.

## 2.4. Kinetic Reactions

The specified rates of the nine reactions involved in the combustion reactor and the gasification reactor are summarized in Table 2 and discussed in the following. Only gasification and combustion phases are considered in the actual Aspen Plus simulation. After pyrolysis, char continues to react with gas. The heterogeneous reactions, modeled by reactions R1–R3 as mentioned in Table 2, are Boudouard, steam gasification, and methanation reactions. The corresponding reaction rate constant is defined by the following expression:  $\text{Reaction rate} = k.T^n.e^{(-E/RT)} \times \text{driving force}$ .

**Table 2.** Kinetic of involved reactions.

Reaction	Equation	Reaction Rate	Reference
R1	$C + CO_2 \rightarrow 2 CO$	$r_1 = 3.42.T.exp(-130000/R.T).[CO_2]$	[25]
R2	$C + H_2O \rightarrow CO + H_2$	$r_2 = 3.42.T.exp(-130000/R.T).[H_2O]$	[25]
R3	$C + 2H_2 \rightarrow CH_4$	$r_3 = 0.00342.T.exp(-130000/R.T).[H_2]$	[25]
R4	$CO + H_2O \rightarrow CO_2 + H_2$	$r_4 = 7.68 \times 10^{10}.exp(-304600/R.T).[CO]^{0.5}.[H_2O]$	[26]
R5	$CO_2 + H_2 \rightarrow CO + H_2O$	$r_5 = 6.4 \times 10^9.exp(-326400/R.T).[H_2]^{0.5}.[CO_2]$	[26]
R6	$CH_4 + H_2O \rightarrow CO + 3H_2$	$r_6 = 3 \times 10^8.exp(-125000/R.T).[CH_4].[H_2O]$	[27]
R7	$H_2 + 0.5 O_2 \rightarrow H_2O$	$r_7 = 1.63 \times 10^{11}.T^{-1.5}.exp(-28500/R.T).[O_2].[H_2]^{1.5}$	[28]
R8	$CO + 0.5 O_2 \rightarrow CO_2$	$r_8 = 5.62 \times 10^{12}.exp(-133000/R.T).[O_2]^{0.5}.[CO]$	[28]
R9	$CH_4 + 2 O_2 \rightarrow CO_2 + 2H_2O$	$r_9 = 3.552 \times 10^{11}.exp(-130529/R.T).[O_2].[CH_4]$	[28]

Regarding modeling of heterogeneous gasification reactions, it is stated in the literature that it depends on the homogeneous gas phase reaction model as it depends on the surrounding gas species [25,29]. The reaction rate expressions for the heterogeneous reactions are the same as for the homogeneous reactions.

## 3. Validation

Due to a lack of experimental data for *Prosopis juliflora* gasification in fluidized bed, the feedstock used to validate the model is wood pellets ( $CH_{1.4}O_{0.64}$ )<sub>33</sub> which is used by Campoy et al. [30]. A comparison with their experimental data from air–steam gasification of wood pellets in a bubbling fluidized bed reactor is analyzed. A comparison with numerical data of Beheshti et al.'s [18] Aspen Plus model is made as well. Correlations are used for predicting devolatilization products.

Campoy et al. [30] used wood pellets as fuel and ofite, which is a silicate subvolcanic rock with formula  $(Ca, Mg, Fe, Ti, Al)_2(SiAl)_2O$  that has a density of 2650 kg/m<sup>3</sup>, as bed material. They considered air and air with steam as gasification agents. The stoichiometric ratio (SR) and steam to biomass ratio (SBR) ranged from 0.19 to 0.35 and from 0 to 0.45, respectively, by changing both the vapor flow rate (from 0 to 5.1 kg/h) and the biomass flow rate (from 12.2 to 20.5 kg/h) while retaining an approximately steady air flow rate (from 17 Nm<sup>3</sup>/h). The operating temperature ranged between 730 °C and 815 °C. Table 3 describes the pilot plant's most critical parameters, under the terms of the research experiments. Details of the gasifier plant and different input parameters can be found in their work [30].

**Table 3.** Technical and operating parameters of the Campoy et al.'s [30] pilot plant.

Parameter	Value
Inside diameter of the bed	0.15 m
Inside diameter of the freeboard	0.25 m
Height of the bed	1.40 m
Height of the freeboard	2.15 m
Fuel flow rate	12–21 kg/h



Table 4 displays the LHV of the syngas in addition to its composition. It shows that the model results are in good agreement with Campoy et al. [30] and Beheshti et al.'s [18] findings. More specifically, the present model presents syngas composition's percentages close to the existed data. Percentages were closer to the experimental ones [30] than those of Beheshti et al.'s [18] values. The LHV calculated by the present model was found to be 6.699 MJ/Nm<sup>3</sup> and showed a good agreement with the experimental value as well, which was found to be 4.76 MJ/Nm<sup>3</sup>.

**Table 4.** Lower heating value (LHV) and composition of the syngas.

Model	LHV (MJ/Nm <sup>3</sup> )	Syngas Composition (%Vol, Dry, Free N <sub>2</sub> )			
		CO	CH <sub>4</sub>	H <sub>2</sub>	CO <sub>2</sub>
Model (Present work)	6.699	33.51	9.26	18.25	38.96
Experimental (Campoy et al. [30])	4.76	35.3	11.4	19.5	33.8
Model (Beheshti et al. [18])	-	37.2	14.25	17.4	31.15

#### 4. Results and Discussions

The volume of the combustion reactor is set at  $V_{\text{comb}} = 0.3 \text{ m}^3$ , while the diameter of gasification reactor changes from 0.35 m to 0.55 m. The maximum height of the gasifier is between 2 m and 4 m. The biomass *Prosopis juliflora* mass flow is 10 kg/h. With respect to Chandrasekaran analysis [21], this mass flow gives 6.64 kg/h (char + gas) which represents 66.4% of pyrolysis product of PJ. Char represents approximately 21% and gas represents 45.4% of fuel mass flow. Subsequently, 2.1 kg/h of solid char is assumed to enter the gasifier reactor. A 4.54 kg/h of pyrolytic gas is considered as an input of the combustor reactor considered isothermal at 1000 °C and maintained at 1 bar. The corresponding mass flow of the air varies between 2 and 5 kg/h at 25 °C and is mixed with pyrolytic gas at 600 °C.

In the following, a parametric study of the effect of gasification temperature, air to biomass ratio, and gasifier dimensions (diameter and height) is presented. The composition of syngas and its LHV along with cold gas efficiency (CGE) are the principal studied output variables. In addition, flow regimes in the fluidized gasifier are identified for different bed inventories.

##### 4.1. Effect of Gasifier Temperature

The considered parameters are: air/biomass ratio = 40%, gasifier diameter  $D = 0.5 \text{ m}$ , and gasifier height  $H = 2.5 \text{ m}$ .

##### 4.1.1. Syngas Composition

According to Figure 2a, the CO molar fraction is prevailing and clearly increases with  $T_{\text{gasif}}$ ; however, CO<sub>2</sub> concentration decreases. As a consequence, the LHV of syngas also increases with  $T_{\text{gasif}}$  (Figure 2b). This rising tendency is already mentioned in previous studies for biomass air gasification [7], CO<sub>2</sub> gasification [31], and steam gasification [32] for low steam to biomass ratio. Figure 2a reveals that the production of gases with lower molecular weights is favored by any rise in gasification temperature. Additionally it must be mentioned that the thermodynamic equilibrium model predicts much greater conversion for the Boudouard reaction, causing considerably higher carbon monoxide concentrations and consistently lower carbon dioxide values [31].

No considerable increase in CO concentration is observed for  $T_{\text{gasif}}$  greater than 900 °C. The absence of steam in the gasifier may be noted. Supplementary simulations with injection of steam inside the gasifier (easily to introduce in “fluidbed” block) show that H<sub>2</sub> molar fraction increases with  $T_{\text{gasif}}$ ; however, the concentration of CH<sub>4</sub> decreases. This behavior is well confirmed in the literature [28]. Recently Lan et al. [33] presented a comparison between fluidized bed biomass gasification with and without steam. With the addition of steam and as the bed temperature increased, gas reforming reactions rose, and the CO and CH<sub>4</sub> content diminished; however, CO<sub>2</sub> and H<sub>2</sub> content went up.

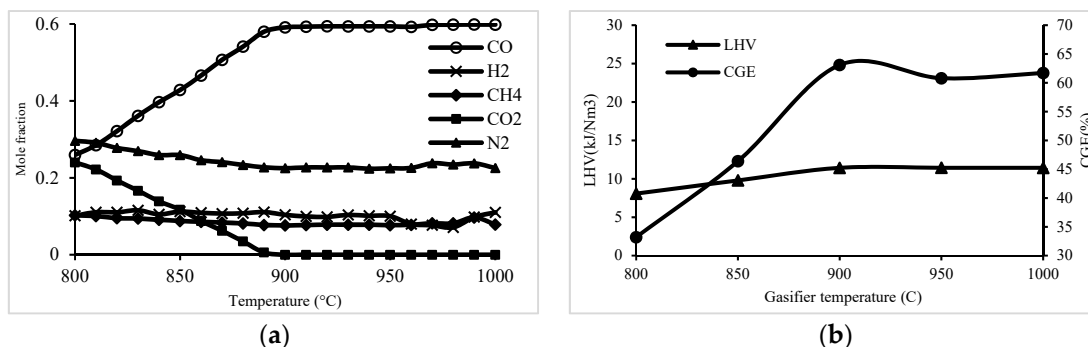


**Figure 2.** Effect of the gasifier temperature on (a) syngas composition and (b) LHV and cold gas efficiency (CGE).

#### 4.1.2. LHV and CGE

The increasing tendency in Figure 2b is directly related to producer gas composition for different gasifier temperatures (Figure 2a). Figure 2b shows that  $T_{\text{gasif}} = 900$  °C gives a satisfactory LHV of syngas (11.43 MJ/Nm<sup>3</sup>) and maximal cold gas efficiency CGE (63%) of the entire gasifier. This promising LHV value is relatively high for air biomass gasification even for low air/biomass ratio.

#### 4.2. Effect of Air/Biomass Ratio

The considered parameters are:  $T_{\text{gasif}} = 900$  °C, gasifier diameter  $D = 0.5$  m, and gasifier height  $H = 2.5$  m.

##### 4.2.1. Syngas Composition

Figure 3a shows a remarkable N<sub>2</sub> rate increase for higher air/biomass ratios. As predicted a rise in CO<sub>2</sub> molar fraction and a reduction in CO fraction are observed.

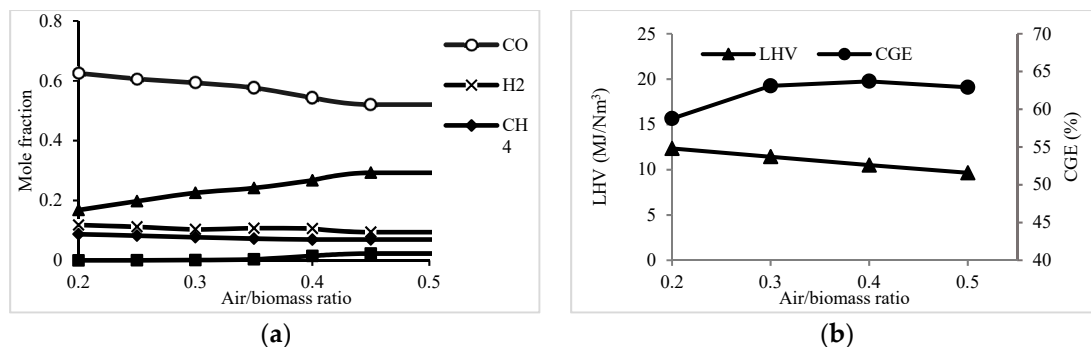


**Figure 3.** Effect of the equivalence ratio on (a) the gas composition and (b) the LHV and CGE.

#### 4.2.2. LHV and CGE

Figure 3b shows a decreasing trend of LHV when air/biomass ratio increases. The principal reason for this behavior is the combustion reactions happening in the combustor for a greater air flow rate. This is confirmed in Figure 4 showing gas composition at the output of the combustor. For air mass rate near 5 kg/h, all CO is oxidized leading to an increase in CO<sub>2</sub> fraction. H<sub>2</sub>O is also completely consumed due to the favored water gas shift direct reaction (R5) at high temperature.

According to Figure 3b, the maximum of CGE (63.7%) is obtained for the equivalence ratio of 0.4 (i.e., air mass flow equal to 4 kg/h). The corresponding LHV value is 10.5 MJ/Nm<sup>3</sup>. Indeed, despite the diminishing of LHV with rising air/biomass ratio, the CGE would first increase owing to the growing volume of carbon transformed into gaseous products and then decline due to the dominant effect of the N<sub>2</sub> dilution of the producer gas. With the increase of air/biomass ratio, the quantity of the



oxygen brought to the combustion reactor increases. The gas components of pyrolytic gas burn inside the combustor in the situation of oxygen enrichment and the content of combustible gas is reduced. Accordingly, the temperature increases in the combustion reactor. Nevertheless, the rise in temperature is advantageous to the gasification reactions occurring inside the gasifier. Alternatively, the biomass gas concentration is diluted significantly. Consequently, the increase of air/biomass ratio has a mutual effect on the rise and decline of the combustible gas content in the producer gas. Nevertheless, this analysis is not totally adequate for isothermal combustion and gasification reactors.

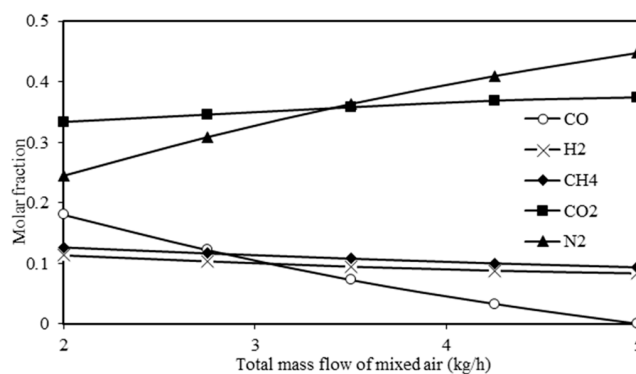


Figure 4. Composition of gas leaving the combustor.

To analyze and evaluate this rate of 4 kg/h of air mass flow, one can focus on the combustor reactor and calculate the corresponding equivalence ratio  $ER_{comb}$ . According to equations R1-R7, one mole of the pyrolytic gas (PYRGAS) consumes 0.6225 mole of  $O_2$  in stoichiometric combustion. Considering a rate of 21% of oxygen in the air, one gets 3.635 kg (air)/kg (pyrolytic-gas) as stoichiometric ratio. Having  $4/4.54 = 0.881$  kg (air)/kg (pyrolytic-gas) as real ratio, one gets the equivalence ratio:  $ER_{comb} = 0.24$  which is inside the literature suggested interval [4]. It is to be noted that the global equivalence ratio corresponding to the combustion of 10 kg of *Proposis juliflora* ( $CH_{0.138}O_{0.978}N_{0.043}$  [21]) with 4 kg/h of air mass flow is equal to 0.13. However, this ratio is not so significant because almost zero oxygen reaches the gasification reactor and so no oxidation of char is predicted.

#### 4.3. Effect of Gasifier Diameter

The fixed parameters are: mass flow air/biomass ratio = 40%, gasifier temperature  $T_{gazif} = 900$  °C, and gasifier height  $H = 2.5$  m. Figure 5a shows a promising effect of increasing gasifier diameter on gas composition. In fact, for a larger diameter, the height of bottom zone is lower and the freeboard height is bigger. In addition, the minimum fluidization velocity decreases. All these changes in flow regimes favor gasification reactions.

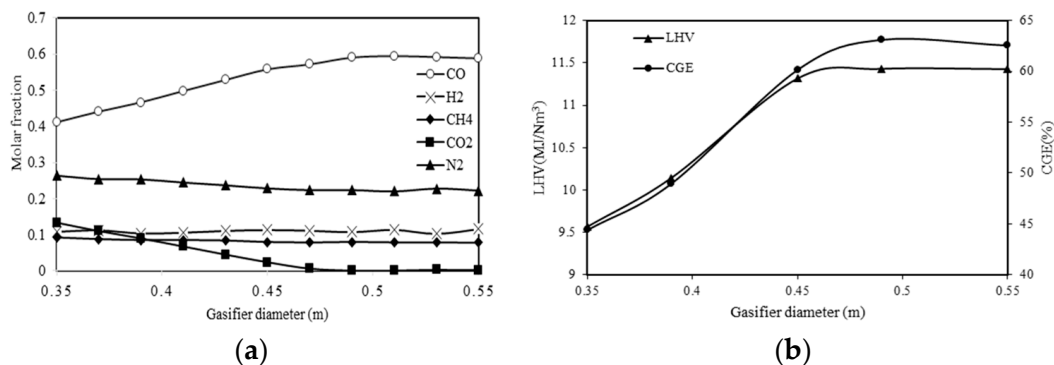


Figure 5. Effect of the gasifier diameter on: (a) the gas composition, (b) the LHV and CGE.

This is confirmed in Figure 5b where the rise in the LHV of syngas is significant between 0.35 m and 0.45 m. Figure 5b shows an analogous behavior of CGE. It may be noted that a maximum value of the cold gas efficiency is about 63.1% for  $D = 0.49$  m. Consequently, the diameter of 0.5 m is proposed for this multistage gasifier.

#### 4.4. Effect of Gasifier Height

The considered parameters are:  $T_{\text{gazif}} = 900$  °C, gasifier diameter  $D = 0.5$  m, and mass flow air to biomass ratio equals 40%.

From Figure 6 the height of 2.5 m of the gasifier is adequate for the choice of a good quality of syngas and consequently for LHV and CGE. From 2.5 m to 4 m no considerable variation is observed. This behavior is linked to the flow regime in the gasifier as discussed in the following section. It may be noted that the performance area rate is still the same for all values of  $H$ .

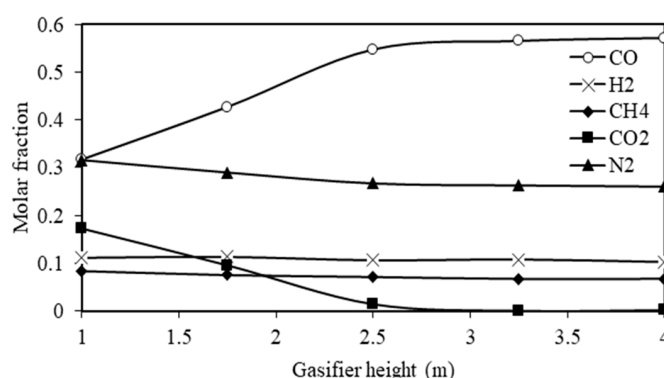


Figure 6. Gas composition along the gasifier height.

#### 4.5. Flow Regimes in the Gasifier—Effect of Bed Inventory

In order to recognize different flow regimes inside the gasifier, three initial bed masses of 50, 100, and 150 kg are considered. Table 5 summarizes parameters and results for three different bed masses of char (carbon solid). For 100 kg and 150 kg inventory, the bottom bed has a bubbling fluidized nature and the freeboard is a supplementary dilute zone. In the case of a 50 kg bed mass, there is almost 0 m of bubbling bed height. Figure 7a, showing distribution of solid volume fraction, confirms these results. In addition, the distributions of pressure and superficial velocity in the gasifier confirm these bubbling or totally fluidized bed behaviors (Figure 7b,c). Regarding the superficial velocity displayed in Figure 7c, there is no significant difference between the three beds' inventories, due to the fact that the same air mass flow was introduced in all three cases. It can be observed that the superficial velocity increased with the increase of the gasifier height which is related to the formation of bubbles in the bed, causing solid particles detachment. It increases more in the freeboard zone. A slight difference can be observed in the freeboard region between the superficial velocities of the three beds' inventories.

Table 5. Bed parameters for the three mass inventories 50, 100, and 150 kg.

Bed Inventory (kg)	50	100	150
Bottom zone height (m)	0	0.171	0.416
Freeboard height (m)	2.499	2.328	2.083
Distributor pressure drop (mbar)	3.986	3.986	3.986
Bottom zone pressure drop (mbar)	0.0015	17.36	42.23
Freeboard pressure drop (mbar)	32.31	32.63	32.73
Overall pressure drop (mbar)	36.307	53.99	78.956
Minimum fluidization velocity (cm/sec)	0.3547	0.3558	0.3564

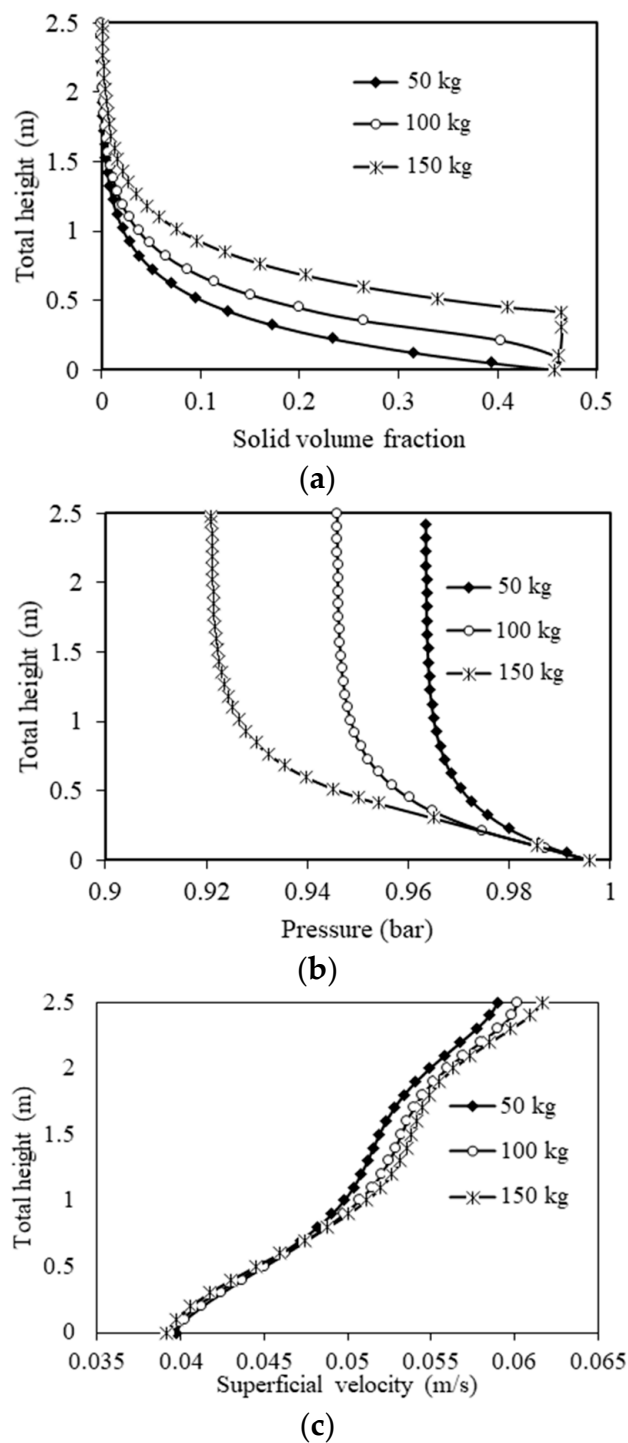


**Figure 7.** (a) Solid volume fraction distributions, (b) pressure distribution, and (c) superficial velocity, along the gasifier for a bed mass inventory of 50 kg, 100 kg, and 150 kg.

A close depiction of Figure 8 shows an increase in CO molar fraction and a decrease in CO<sub>2</sub> molar fraction inside the gasifier. The same behavior is observed by Cheng et al. [24]. A linear variation of gas component fraction in the bottom zone is observed. In the splash region a constant behavior is observed and particularly no variation on CO and CO<sub>2</sub> molar fractions in the height between 1.2 to 1.5 m. This is closely linked to the constant behavior of superficial velocity in this region (Figure 8c).

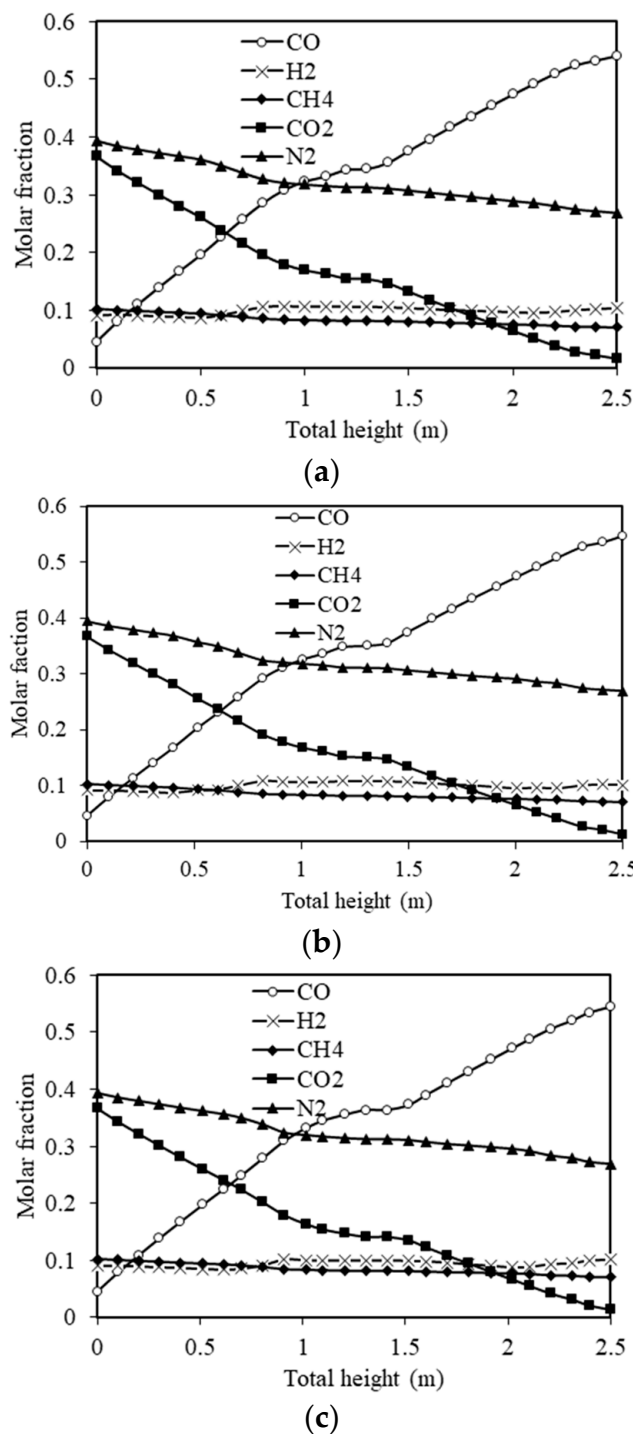


**Figure 8.** Gas composition inside the gasifier for a bed mass inventory of (a) 50 kg, (b) 100 kg, and (c) 150 kg.

## 5. Conclusions

An Aspen plus model is proposed to simulate air gasification of *Prosopis juliflora*. The gasification system is a multistage reactor with different compartments for pyrolysis, combustion, and reduction that takes place in a fluidized bed. The gasifier design studied in this work aims to generate a high-quality product gas. The numerical modeling considered in this work is based on a semi-detailed kinetic approach that considers both reaction rates and hydrodynamic parameters. It could be used to optimize the gasifier performances by the design and the operating conditions. Simulations revealed that the

most influential parameters are the temperature of gasification reactor and the air to biomass mass ratio. Results showed that CO concentration in the product gas is proportional to gasifier temperature and inversely proportional to air to biomass ratio. The bed inventory has great influence on flow regimes inside the gasifier. An optimal elevated LHV value ( $10.53 \text{ MJ/Nm}^3$ ) is obtained for 2 m gasifier height, 0.5 m diameter, and an equivalence ratio in the combustor equal to 0.24. The corresponding cold gas efficiency is about 65%. Consequently, this new multistage reactor produces a high gas calorific value even with air gasification and with monoxide as a main component. This Aspen model can be easily adapted for other biomass substances. Future simulations will take account of the presence of tar in the pyrolytic gas. Ongoing tests consider naphthalene, toluene, phenol, and benzene as principal tar components.

**Author Contributions:** Conceptualization, M.D. and W.H.; methodology, L.K. and M.N.B.; software, K.G. and C.M.; validation, M.D., K.G., and W.H.; formal analysis, L.K. and M.N.B.; investigation, K.G. and M.D.; resources, K.G.; writing—original draft preparation, M.D., W.H., and M.N.B.; writing—review and editing, L.K. and M.D.; supervision, M.N.B.; project administration, K.G.; funding acquisition, K.G. All authors have read and agreed to the published version of the manuscript.

**Funding:** This research was funded by the Deanship of Scientific Research at Princess Nourah bint Abdulrahman University through the Fast-track Research Funding Program.

**Acknowledgments:** This work was undertaken with the support of the Tunisian ministry of higher education and research in the framework of the Tunisian-Indian cooperation in scientific research and technology.

**Conflicts of Interest:** The authors declare no conflict of interest.

## Nomenclature

CGE	Cold Gas Efficiency	
D	Diameter	(m)
ER	Equivalence Ratio	
H	Height	(m)
HHV	High Heating Value	(MJ/Nm <sup>3</sup> )
k	Kinetic factor	
LHV	Low Heating Value	(MJ/Nm <sup>3</sup> )
$\dot{m}$	Mass flow	(kg s <sup>-1</sup> )
P	Pressure	(Pa)
PJ	<i>Prosopis juliflora</i>	
r	Reaction rate	
S <sub>v</sub>	Volume-specific surface area	(m <sup>3</sup> )
T	Temperature	(°C)
t	Time	(s)
u	Velocity	(m s <sup>-1</sup> )
V	Volumetric flow	(m <sup>3</sup> s <sup>-1</sup> )
<b>Greek symbols:</b>		
$\varepsilon$	Bed porosity	
$\varepsilon_b$	Local bubble volume fraction	
$\gamma$	Viscosity	(kg m <sup>-1</sup> s <sup>-1</sup> )
$\rho$	Density	(kg m <sup>-3</sup> )
<b>Subscripts:</b>		
dis	Distributor	
g	Gas	
gasif	Gasification	
mf	Minimum fluidization	
or	Orifice	

## References

1. Jankes, G.G.; Trninić, M.R.; Stamenić, M.S.; Simonović, T.S.; Tanasić, N.T.; Labus, J.M. Biomass gasification with CHP production: A review of state of the art technology and near future perspectives. *Therm. Sci.* **2012**, *16*, 115–130. [CrossRef]
2. Jingjing, L.; Xing, Z.; DeLaquil, P.; Larson, E.D. Biomass energy in China and its potential. *Energy Sustain. Dev.* **2001**, *5*, 66–80. [CrossRef]
3. Begum, S.; Rasul, M.G.; Akbar, D.; Ramzan, N. Performance analysis of an integrated fixed bed gasifier model for different biomass feedstocks. *Energies* **2013**, *6*, 6508–6524. [CrossRef]
4. Basu, P. *Biomass Gasification and Pyrolysis: Practical Design and Theory*; Academic Press: Cambridge, MA, USA, 2010.
5. Janković, B.Ž.; Radojević, M.B.; Balać, M.M.; Stojiljković, D.D.; Manić, N.G. Thermogravimetric study on the pyrolysis kinetic mechanism of waste biomass from fruit processing industry. *Therm. Sci.* **2020**, *24*, 4221–4239. [CrossRef]
6. Loha, C.; Gu, S.; de Wilde, J.; Mahanta, P.; Chatterjee, P.K. Advances in mathematical modeling of fluidized bed gasification. *Renew. Sustain. Energy Rev.* **2014**, *40*, 688–715. [CrossRef]
7. Antonopoulos, I.-S.; Karagiannidis, A.; Elefsiniotis, L.; Perkoulidis, G.; Gkouletsos, A. Development of an innovative 3-stage steady-bed gasifier for municipal solid waste and biomass. *Fuel Process. Technol.* **2011**, *92*, 2389–2396. [CrossRef]
8. Choi, Y.-K.; Ko, J.-H.; Kim, J.-S. A new type three-stage gasification of dried sewage sludge: Effects of equivalence ratio, weight ratio of activated carbon to feed, and feed rate on gas composition and tar, NH<sub>3</sub>, and H<sub>2</sub>S removal and results of approximately 5 h gasification. *Energy* **2017**, *118*, 139–146. [CrossRef]
9. Valderrama Rios, M.L.; González, A.M.; Lora, E.E.S.; Almazán del Olmo, O.A. Reduction of tar generated during biomass gasification: A review. *Biomass Bioenergy* **2018**, *108*, 345–370. [CrossRef]
10. Kundsén: Experience with ASPEN while Simulating a New Methanol Plants. Available online: [https://scholar.google.com/scholar\\_lookup?title=Experience%20with%20ASPEN%20while%20simulating%20a%20new%20methanol%20plant&author=R.A.%20Kundsén&publication\\_year=1982](https://scholar.google.com/scholar_lookup?title=Experience%20with%20ASPEN%20while%20simulating%20a%20new%20methanol%20plant&author=R.A.%20Kundsén&publication_year=1982) (accessed on 17 June 2019).
11. Mallick, D.; Buragohain, B.; Mahanta, P.; Moholkar, V.S. Gasification of mixed biomass: Analysis using equilibrium, semi-equilibrium, and kinetic models. In *Coal and Biomass Gasification: Recent Advances and Future Challenges*; De, S., Agarwal, A.K., Moholkar, V.S., Thallada, B., Eds.; Springer: Berlin/Heidelberg, Germany, 2018; pp. 223–241.
12. Damartzis, T.; Michailos, S.; Zabaniotou, A. Energetic assessment of a combined heat and power integrated biomass gasification–internal combustion engine system by using Aspen Plus®. *Fuel Process. Technol.* **2012**, *95*, 37–44. [CrossRef]
13. Nikoo, M.B.; Mahinpey, N. Simulation of biomass gasification in fluidized bed reactor using Aspen Plus®. *Biomass Bioenergy* **2008**, *32*, 1245–1254. [CrossRef]
14. Niu, M.; Huang, Y.; Jin, B.; Wang, X. Simulation of syngas production from municipal solid waste gasification in a bubbling fluidized bed using Aspen Plus®. *Ind. Eng. Chem. Res.* **2013**, *52*, 14768–14775. [CrossRef]
15. Doherty, W.; Reynolds, A.; Kennedy, D. Aspen Plus® Simulation of Biomass Gasification in a Steam Blown Dual Fluidised Bed. In *BookBook Chapters*; Méndez-Vilas, A., Ed.; Dublin Institute of Technology: Dublin, Ireland, 2013.
16. Sreejith, C.C.; Muraleedharan, C.; Arun, P. Performance prediction of steam gasification of wood using an Aspen Plus® thermodynamic equilibrium model. *Int. J. Sustain. Energy* **2014**, *33*, 416–434. [CrossRef]
17. Mitta, N.R.; Ferrer-Nadal, S.; Lazovic, A.M.; Parales, J.F.; Velo, E.; Puigjaner, L. Modelling and Simulation of a Tyre Gasification Plant for Synthesis Gas Production. In *Computer Aided Chemical Engineering*; Marquardt, W., Pantelides, C., Eds.; Elsevier: Amsterdam, The Netherlands, 2006; Volume 21, pp. 1771–1776.
18. Beheshti, S.M.; Ghassemi, H.; Shahsavan-Markadeh, R. Process simulation of biomass gasification in a bubbling fluidized bed reactor. *Energy Convers. Manag.* **2015**, *94*, 345–352. [CrossRef]
19. Abdelouahed, L.; Authier, O.; Mauviel, G.; Corriou, J.P.; Verdier, G.; Dufour, A. Detailed modeling of biomass gasification in dual fluidized bed reactors under Aspen Plus®. *Energy Fuels* **2012**, *26*, 3840–3855. [CrossRef]
20. Dhrioua, M.; Hassen, W.; Kolsi, L.; Anbumalar, V.; Alsagri, A.S.; Borjini, M.N. Gas distributor and bed material effects in a cold flow model of a novel multi-stage biomass gasifier. *Biomass Bioenergy* **2019**, *126*, 14–25. [CrossRef]



21. Chandrasekaran, A.; Ramachandran, S.; Subbiah, S. Modeling, experimental validation and optimization of prosopis juliflora fuelwood pyrolysis in fixed-bed tubular reactor. *Bioresour. Technol.* **2018**, *264*, 66–77. [[CrossRef](#)] [[PubMed](#)]
22. Eri, Q.; Peng, J.; Zhao, X. CFD simulation of biomass steam gasification in a fluidized bed based on a multi-composition multi-step kinetic model. *Appl. Therm. Eng.* **2018**, *129*, 1358–1368. [[CrossRef](#)]
23. Snider, D.M.; Clark, S.M.; O'Rourke, P.J. Eulerian–lagrangian method for three-dimensional thermal reacting flow with application to coal gasifiers. *Chem. Eng. Sci.* **2011**, *66*, 1285–1295. [[CrossRef](#)]
24. Gómez-Barea, A.; Leckner, B. Modeling of biomass gasification in fluidized bed. *Prog. Energy Combust. Sci.* **2010**, *36*, 444–509. [[CrossRef](#)]
25. Xie, J.; Zhong, W.; Jin, B.; Shao, Y.; Liu, H. Simulation on gasification of forestry residues in fluidized beds by eulerian–lagrangian approach. *Bioresour. Technol.* **2012**, *121*, 36–46. [[CrossRef](#)]
26. Geldart, D. Types of gas fluidization. *Powder Technol.* **1973**, *7*, 285–292. [[CrossRef](#)]
27. Hussain, M.; Tufa, L.D.; Yusup, S.; Zabiri, H. A kinetic-based simulation model of palm kernel shell steam gasification in a circulating fluidized bed using Aspen Plus®: A case study. *Biofuels* **2018**, *9*, 635–646. [[CrossRef](#)]
28. Cheng, Y.; Thow, Z.; Wang, C.-H. Biomass gasification with CO<sub>2</sub> in a fluidized bed. *Powder Technol.* **2016**, *296*, 87–101. [[CrossRef](#)]
29. Gerber, S.; Behrendt, F.; Oevermann, M. An eulerian modeling approach of wood gasification in a bubbling fluidized bed reactor using char as bed material. *Fuel* **2010**, *89*, 2903–2917. [[CrossRef](#)]
30. Campoy, M.; Gómez-Barea, A.; Vidal, F.B.; Ollero, P. Air–steam gasification of biomass in a fluidised bed: Process optimisation by enriched air. *Fuel Process. Technol.* **2009**, *90*, 677–685. [[CrossRef](#)]
31. Sadhwani, N.; Li, P.; Eden, M.R.; Adhikari, S. Process Modeling of Fluidized Bed Biomass-CO<sub>2</sub> Gasification using ASPEN Plus®. In *Computer Aided Chemical Engineering*; Espuña, A., Graells, M., Puigjaner, L., Eds.; Elsevier: Amsterdam, The Netherlands, 2017; Volume 40, pp. 2509–2514.
32. Pala, L.P.R.; Wang, Q.; Kolb, G.; Hessel, V. Steam gasification of biomass with subsequent syngas adjustment using shift reaction for syngas production: An Aspen Plus® model. *Renew. Energy* **2017**, *101*, 484–492. [[CrossRef](#)]
33. Lan, W.; Chen, G.; Zhu, X.; Wang, X.; Xu, B. Research on the characteristics of biomass gasification in a fluidized bed. *J. Energy Inst.* **2019**, *92*, 613–620. [[CrossRef](#)]

**Publisher's Note:** MDPI stays neutral with regard to jurisdictional claims in published maps and institutional affiliations.



© 2020 by the authors. Licensee MDPI, Basel, Switzerland. This article is an open access article distributed under the terms and conditions of the Creative Commons Attribution (CC BY) license (<http://creativecommons.org/licenses/by/4.0/>).